ANALELE UNIVERSITĂȚII
"EFTIMIE MURGU" REȘIȚA
ANUL XX, NR. 2, 2013, ISSN 1453 - 7397

Tiberiu Mănescu Jr., Gilbert-Rainer Gillich, Ion Dumitru, Lorand Kun

Considerations on the Approach of Rolling Contact Fatigue Assuming Multiaxial States of Stress

Rolling contact fatigue appears in many mechanical elements, in the presence of variable local loadings. During the last years an increasing attention has been awarded macroscopic and mesoscopic analysis of repetitive rolling contact, taking into consideration local triaxial states of stress. Given the above, the authors analyze a fatigue criterion based on the stress state invariants, which is validated using original results as well as existing data from the literature. The criterion is applied to the case of linear contact with friction, which has analytical solutions for the elastic state of stress on the rolling surface and in the adjacent zone. A durability calculation method is presented for the case of rolling contact, based on the ratio between the maximum and experimentally obtained critical (limit) value of a damage parameter.

Keywords: *rolling contact, bearing, multiaxial fatigue, stress invariants*

1. General approach of rolling contact fatigue

Repetitive rolling contact is the main cause of several mechanical elements failures, such as: bearing balls, gear wheels, cams and generally any rolling elements.

The surfaces exposed to repetitive rolling contact suffer a degradation which is variously denoted in the literature. Thus, Tallian considers that this degradation manifests itself through spalling [1]. Other authors denote the phenomenon as follows: pitting, flaking, micro-pitting or generally contact fatigue.

The process of contact fatigue degradation generally has three phases:

- Initial phase, which is short and during which certain in-depth property changes occur in the strongly loaded material;
- A longer second phase, during which the fatigue phenomenon manifests itself at micro level;
- The final phase, during which the micro-cracks grow until they become spalls.

The rolling contact fatigue phenomenon can appear on the contact surface or at a certain depth under it, depending directly on the state of stress, residual stress and the presence of structural discontinuities.

The approach of rolling contact fatigue is particularly complex and is based on the methods of classical theory of elasticity, plasticity, elastic and/or plastic shakedown and ratcheting [2].

The response modeling at plastic shakedown or ratcheting constitutes one of the most complex problems of the theory of plasticity [3][4].

During the last years an increasing attention has been directed towards durability calculation in case of rolling contact, taking into account the triaxial state of stress specific to this kind of loading.

In this context, the authors analyze the opportunity of application of a macroscopic rolling fatigue criterion, based on the stress invariants [5][6].

The above are illustrated for the complex case of a linear rolling contact, taking into consideration the friction forces as well. Based on the applied criterion, a rolling contact fatigue durability evaluation is carried out by reducing the triaxial states of stress to an equivalent uniaxial state, which then is compared with a critical limit state.

2. Stress-state analysis in case of linear rolling contact with friction

The analyzed domain contains the whole width of the contact zone and it concerns volume elements situated on the contact surface as well as at a certain depth under the contact surface (Figure 1).

The analysis of the stress state is based on the analytical solutions given by Liu, which have been transformed into applicable forms for the given conditions [7]:

$$\sigma_{xx} = -\frac{a}{\dfrac{\pi}{\left(1+\dfrac{2}{R_1}\right)\left(1+\dfrac{2}{R_2}\right)}\left(\dfrac{1-\nu_1^2}{E_1}+\dfrac{1-\nu_2^2}{E_1}\right)}\left\{z\left(\frac{a^2+2z^2+2x^2}{a}\Phi_1-\frac{2\pi}{a}-3x\Phi_2\right)+\right.$$
$$\left.+f\left[\left(2x^2-2a^2-3z^2\right)\Phi_2+\frac{2\pi x}{a}+2\left(a^2-x^2-z^2\right)\frac{x}{a}\Phi_1\right]\right\}, \tag{1}$$

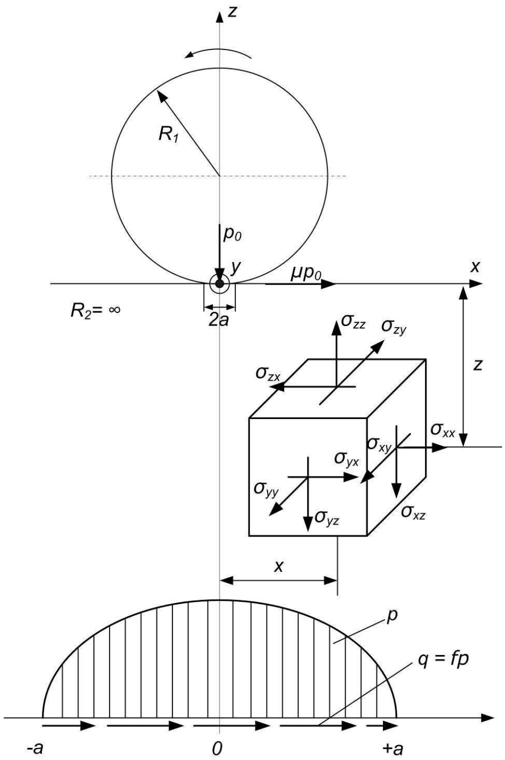

Figure 1. Pressure distribution and state of stress at the linear rolling contact with friction

$$\sigma_{yy} = -\frac{2\nu a}{\frac{\pi}{\left(1+\frac{2}{R_1}\right)\left(1+\frac{2}{R_2}\right)}\left(\frac{1-\nu_1^2}{E_1}+\frac{1-\nu_2^2}{E_1}\right)}\left\{z\left(\frac{a^2+x^2+z^2}{a}\Phi_1-\frac{\pi}{a}-2x\Phi_2\right)+\right. \tag{2}$$

$$\left.+f\left[\left(x^2-a^2-z^2\right)\Phi_2+\frac{\pi x}{a}+\left(a^2-x^2-z^2\right)\frac{x}{a}\Phi_1\right]\right\},$$

$$\sigma_{zz} = -\frac{a}{\frac{\pi}{\left(1+\frac{2}{R_1}\right)\left(1+\frac{2}{R_2}\right)}\left(\frac{1-\nu_1^2}{E_1}+\frac{1-\nu_2^2}{E_1}\right)}\left[z\left(a\Phi_1-x\Phi_2\right)+fz^2\Phi_2\right], \tag{3}$$

$$\sigma_{zx}=-\frac{a}{\frac{\pi}{\frac{1}{2R_1}+\frac{1}{2R_2}}\left(\frac{1-\nu_1^2}{E_1}+\frac{1-\nu_2^2}{E_1}\right)}\left\{z^2\Phi_2+f\left[\left(a^2+2x^2+2z^2\right)\frac{z}{a}\Phi_1-\frac{2\pi z}{a}-3xz\Phi_2\right]\right\}, \quad (4)$$

where:

$$\Phi_1=\frac{\pi\left(\sqrt{(a+x)^2+z^2}+\sqrt{(a-x)^2+z^2}\right)}{\sqrt{\left[(a+x)^2+z^2\right]\left[(a-x)^2+z^2\right]}\sqrt{2\sqrt{\left[(a+x)^2+z^2\right]\left[(a-x)^2+z^2\right]}+2x^2+2z^2-2a^2}} \quad (5)$$

$$\Phi_2=\frac{\pi\left(\sqrt{(a+x)^2+z^2}-\sqrt{(a-x)^2+z^2}\right)}{\sqrt{\left[(a+x)^2+z^2\right]\left[(a-x)^2+z^2\right]}\sqrt{2\sqrt{\left[(a+x)^2+z^2\right]\left[(a-x)^2+z^2\right]}+2x^2+2z^2-2a^2}} \quad (6)$$

a – width of the contact zone;

f – friction coefficient between the roller and the plain;

ν - Poisson's coefficient;

E – tensile modulus of elasticity.

The studied case has the following specific parameters: $R_1 = 7$ *mm*, $R_2 = \infty$, $p_0 = 800$ *N/mm*, ν_1, $\nu_2 = 0.3$, $E_1 = E_2 = 2.1\cdot 10^5$ *MPa*, $f = 0.33$.

Using the equations above, a complete study of the stress state has been carried out on different elements of volume, located on the contact surface as well as at different depths under the contact surface. The stress invariants have been determined as follows:

$$\begin{aligned} I_1 &= \sigma_{xx}+\sigma_{yy}+\sigma_{zz} \\ I_2 &= \sigma_{xx}\sigma_{yy}+\sigma_{xx}\sigma_{zz}+\sigma_{yy}\sigma_{zz}-\sigma_{xz}^2, \\ I_3 &= \sigma_{xx}\sigma_{yy}\sigma_{zz}-\sigma_{yy}\sigma_{xz}^2 \end{aligned} \quad (7)$$

based on which the principal normal stresses σ_1, σ_2 and σ_3 as solutions of the following equations were obtained:

$$\sigma_p^3-I_1\sigma_p^2+I_2\sigma_p-I_3=0 \quad (8)$$

Having the principal normal stresses, the plane positions could be determined defined by the direction cosines l_i, m_i and n_i as solutions of the following equation:

$$\begin{bmatrix} (\sigma_{xx}-\sigma_i) & 0 & \sigma_{xz} \\ 0 & (\sigma_{yy}-\sigma_i) & 0 \\ \sigma_{xz} & 0 & (\sigma_{zz}-\sigma_i) \end{bmatrix}\begin{Bmatrix} l_i \\ m_i \\ n_i \end{Bmatrix}=0 \quad (9)$$

Based on the principal normal stresses, the extreme shear stresses τ_1, τ_2 and τ_3 were also determined.

Figure 2 presents, for the studied case, the principal normal stresses σ_1, σ_2 and σ_3 along the width of the surface contact zone, and figure 3 presents the variations of the extreme shear stresses at a depth of *z = -0.1638 mm*.

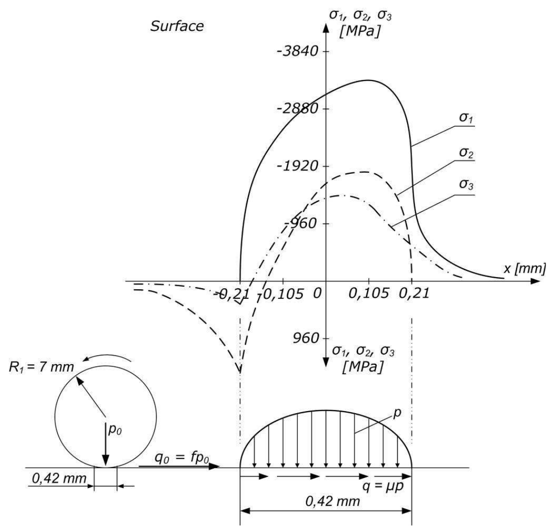

Figure 2. Variation of principal normal stresses along the contact surface width

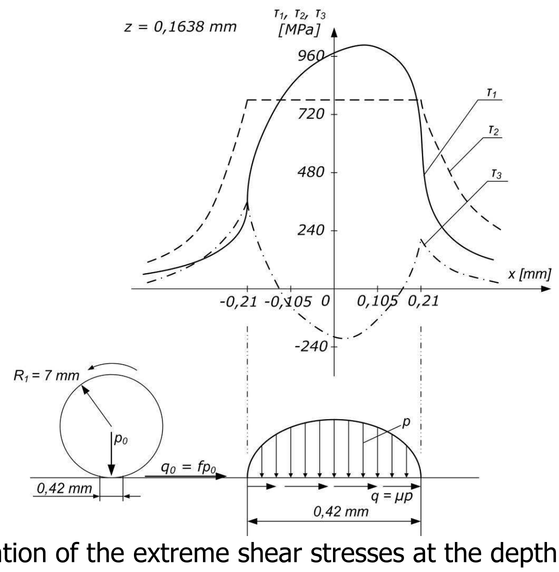

Figure 3. Variation of the extreme shear stresses at the depth *z = 0.1638 mm*

From the above two figures the position of the point on the contact surface can be obtained where all the analyzed parameters reach extreme values.

3. Mathematical model of the damage criterion

In order to determine the durability under rolling contact fatigue conditions, the authors present a criterion based on the stress invariants, which has the following mathematical expression [6][8]:

$$\left[J_{2,am} + \alpha \cdot p_{H,m}^2\right]^{1/2} \le \beta \qquad (10)$$

where:

$J_{2,am}$ is the amplitude of the second invariant of the deviatoric stress tensor, [MPa^2];

p_H is the mean hydrostatic pressure, [MPa];

α, β are material constants which are determined by uniaxial fatigue tests, i.e. fully reversed tension and torsion.

Setting the condition that equation 10 satisfies the parameters of simple fully reversed tension and torsion tests, the constants α, β will be determined and the criterion will become:

$$\left\{J_{2,am} + \left[\left(\frac{3\tau_{-1}}{\sigma_{-1}}\right)^2 - 3\right] p_{H,m}^2\right\}^{1/2} \le \tau_{-1} \qquad (11)$$

where:

σ_{-1} is the fatigue limit at fully reversed tension cycles;

τ_{-1} is the fatigue limit at fully reversed torsion cycles.

The presented calculation method is applicable for steels having $\alpha > 10$ and $\tau_{-1}/\sigma_{-1} > \sqrt{3}/3$.

The left term of the general equation (11) can be considered as an equivalent shear stress, $\tau_{eq} \le \tau_{-1}$. The criterion has been verified using original experimental data obtained by the authors, as well as using based on existing studies from the literature [8][9][10][11][12]. For the case of non-proportional loadings, a polynomial 3rd grade weight function is proposed in order to correct the amplitude of $J_{2,am}$ [6][8].

4. Application of the model for durability study of rolling contact fatigue

The presented model has been applied respecting the loading conditions indicated in paragraph 2, for which the stress state was analyzed on the contact surface and at different depths.

Using the stress tensors calculated on 50 different volume elements on the interval $-a$ and a, the mean hydrostatic pressure was computed, and the amplitude of the deviatoric stress tensor's second invariant was determined. Figure 4 presents the variations of the above two parameters along the width of the contact zone, i.e. *[-a, a]*, according to the rolling surface. Figure 5 shows the variations of the same parameters at a depth of *0.0525* mm under the contact surface.

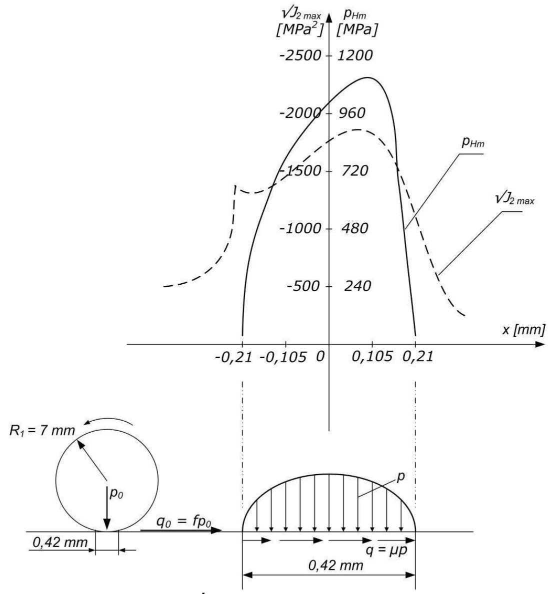

Figure 4. Variation of $\sqrt{J_{2,max}}$ and $p_{H,m}$ on the contact surface

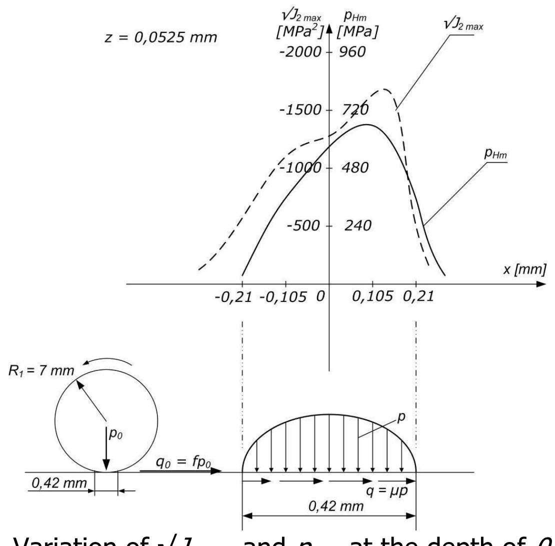

Figure 5. Variation of $\sqrt{J_{2,max}}$ and $p_{H,m}$ at the depth of *0.0525 mm*

In case of all the studied elements of volume the equivalent stresses τ_{eq} have been calculated.

Table 1 indicates the values of the above mentioned equivalent stresses for 21 surface elements and the safety coefficients for fatigue, determined using the ratio c = τ_{-1}/τ_{eq} for a steel having $\tau_{-1} = 900\ MPa$.

Table 1. Equivalent stress values and safety coefficients for rolling contact fatigue

No.	x	p_{Hm}	$\sqrt{J_2}_{max}$	$\sqrt{J_{2,am}}$	$\left[J_{2,am}+\alpha\cdot p_{H,m}^2\right]$	$\dfrac{\tau_{eff}}{\left[J_{2,am}+\alpha\cdot p_{H,m}^2\right]^{1/2}}$
	[mm]	[MPa]	[MPa]	[MPa]	[MPa]	[-]
1	-0.21	-48	660	330	330	2.73
2	-0.189	-256	666	333	336	2.68
3	-0.168	-608	672	336	351	2.56
4	-0.147	-880	690	345	374	2.41
5	-0.126	-1088	714	357	400	2.25
6	-0.105	-1312	744	372	430	2.09
7	-0.084	-1504	768	384	458	1.96
8	-0.063	-1648	792	396	481	1.87
9	-0.042	-1744	810	405	498	1.81
10	-0.021	-1888	828	414	519	1.74
11	0	-1922	840	420	534	1.69
12	0.021	-2064	852	426	547	1.65
13	0.042	-2112	858	429	554	1.63
14	0.063	-2150	864	432	561	1.61
15	0.084	-2177	870	435	566	1.60
16	0.165	-2142	864	432	560	1.61
17	0.126	-2092	858	429	552	1.63
18	0.147	-2000	852	426	540	1.67
19	0.168	-1840	828	414	514	1.75
20	0.189	-1542	732	366	420	2.14
21	0.21	-1216	600	300	362	2.49

According to the proposed procedure, the most exposed surface element to the appearance of the first micro-crack is the one for which the safety coefficient has the lowest value. It is to be noted that in the studied case, the fatigue cracks can not appear not even for element no. 15 (with the lowest safety coefficient), because the fatigue limit of the analyzed material is not reached.

The proposed method can be extended for different depths, leading to the obtaining of a zone repartition where the first fatigue cracks can nucleate, at macroscopic level.

5. Conclusions

The proposed method was successfully applied for any elastic contact loading, for which the stress field on the contact zone and adjacent zone is known.

The experimental studies showed that $\sqrt{J_{2,am}}$ has a decisive role in the nucleation of the first micro-cracks, while the hydrostatic pressure contributes to their propagation.

The model was experimentally verified by tension-torsion and torsion fatigue tests. The method is applicable for bearing fatigue calculation, where under the conditions of elasto-hydro-dynamic lubrication, the fatigue cracks nucleate under the contact surface of bearing rollers and rings.

References

[1] Tallian T.E., *Failure Atlas for Hertz Contact Machine Elements*, ASME Press, 1992.

[2] Alfredsson B., Olsson M.A., *Mechanics for Contact Fatigue*, In: Fatigue 2000 – Fatigue and Durability Assessment of Materials and Structures, Eds. Bache P.A., Blackmore J., Draper J., Edwalds J.H., Roberts P., Yales J.R., Cambridge, April 10-12, 2000, Chamelion Press Ltd. London.

[3] Jiang Y., Xu B., Sehitoglu H., *Three-dimensional elastic-plastic stress analysis of rolling contact*, Journal of Tribology, 200, 2002, 699-708.

[4] Ekberg A., Kabo E., *Fatigue under rolling contact and thermal loading – an overview*, Wear 258, 2005, 1288-1300.

[5] Dumitru I., Kun L., *On the multiaxial high cycle fatigue damage parameters*, Buletinul Universitatii Petrol-Gaze din Ploiesti, Seria Tehnica, vol. LXIII, nr. 1, 2011, 117-126.

[6] Kun L., Dumitru I., Cotuna E., *A study on multiaxial high cycle fatigue models*, Proceedings of the 15th International ModTech Conference, Chisinau, vol I., 24-24 May 2011, 561-564.

[7] Smith J.O., Liu C.K., *Stress due tangential and normal loads on an elastic solid with application to some contact stress problems*, ASME, Journal of applied mechanics, 20, 1953, 1953.

[8] Kun L., *Modelling and Simulation of Multiaxial Fatigue*, PhD Thesis, Politehnica University of Timisoara, 2012.
[9] Nishihara T., Kawamoto M., *The strength of metals under combined loading and twisting with phase difference*, Memoirs of the College of Engineering, Kyoto University, vol. 9, 1945, 85-112.
[10] Lemmp W., *Strength behavior of steel under multiaxial long life fatigue loading consisting of stresses with superimposed shear stress both in-phase and out-of-phase*, PhD Thesis, University of Stuttgart, 1977.
[11] Sonsino C.M., *Schwingfestigkeitsverhalten von Sinterstahl unter kombinierten mehrachsigen phasengleichen und phasenverschobenen Beanspruchungszustanden*, Bericht Nr. FB-168, Fraunhofer Institut fur Betriebsfestigkeit LBF, Darmstadt, Germany, 1983.
[12] Froustey G., Lasserre S., *Multiaxial fatigue endurance of 30NDC16 steel*, International Journal of Fatigue, vol 11(3), 1989, 169-175.

Addresses:

- Eng. Tiberiu Mănescu Jr., "Eftimie Murgu" University of Reşiţa, Piaţa Traian Vuia, nr. 1-4, 320085, Reşiţa, tibisb01@yahoo.de
- Prof. Dr. Eng. Gilbert-Rainer Gillich, "Eftimie Murgu" University of Reşiţa, Piaţa Traian Vuia, nr. 1-4, 320085, Reşiţa, gr.gillich@uem.ro
- Prof. Dr. Eng. Ion Dumitru, "Politehnica" University of Timişoara, Piaţa Victoriei nr. 2, 300006 Timişoara, dion@mec.upt.ro
- Dr. Eng. Lorand Kun, National R&D Institute for Welding and Material Testing – ISIM Timişoara, Bulevardul Mihai Viteazul nr. 30, 300222 Timişoara, lkun@isim.ro